

Exercise intervention increases expression of bone morphogenetic proteins and prevents the progression of cartilage-subchondral bone lesions in a post-traumatic rat knee model

(ラット外傷性変形性膝関節症モデルに対する運動介入は骨形成蛋白の発現を増大させ関節軟骨 - 軟骨下骨病変の進行を予防する)

飯島 弘貴

Osteoarthritis and Cartilage



Exercise intervention increases expression of bone morphogenetic proteins and prevents the progression of cartilage-subchondral bone lesions in a post-traumatic rat knee model



H. Iijima †‡, T. Aoyama §, A. Ito ‡||, J. Tajino †, S. Yamaguchi †‡, M. Nagai ¶, W. Kiyon †, X. Zhang †, H. Kuroki †*

† Department of Motor Function Analysis, Human Health Sciences, Graduate School of Medicine, Kyoto University, Kyoto, Japan

‡ Japan Society for the Promotion of Science, Tokyo, Japan

§ Department of Development and Rehabilitation of Motor Function, Human Health Sciences, Graduate School of Medicine, Kyoto University, Kyoto, Japan

|| Department of Orthopaedic Surgery, Graduate School of Medicine, Kyoto University, Kyoto, Japan

¶ Congenital Anomaly Research Center, Graduate School of Medicine, Kyoto University, Kyoto, Japan

ARTICLE INFO

Article history:

Received 28 September 2015

Accepted 10 January 2016

Keywords:

Osteoarthritis

Cartilage

Bone micro-CT

Exercise

Bone morphogenetic protein

SUMMARY

Objective: This study aimed to determine whether treadmill walking (TW) prevents the progression of post-traumatic osteoarthritic changes in cartilage-subchondral bone unit, and whether the exercise timing changes the exercise efficacy in destabilized medial meniscus (DMM) rat knees.

Design: Twelve-week-old male Wistar rats underwent DMM surgery on their right knees and sham surgery on their left knees and were assigned to either the sedentary ($n = 10$) or walking ($n = 24$) groups. The rats in the walking group were subjected to TW from day 2 through 4 weeks, from 4 through 8 weeks, or from day 2 through 8 weeks ($n = 8$ per group). Osteoarthritic changes of cartilage and subchondral bone were assessed with micro-computed tomography, histology, and immunohistochemistry 8 weeks after surgery.

Results: TW prevented the progression of cartilage and subchondral bone lesions induced by the DMM, and increased bone morphogenetic protein (BMP)-2 and -6 expressions in superficial zone chondrocytes and bone-lining cells including osteoblasts. Furthermore, the TW-induced increase in BMPs varied with the exercise timing. Beginning TW 4 weeks after DMM surgery was the best option for increasing BMPs, coinciding with the most robust prevention of osteoarthritic changes.

Conclusions: TW increased the expression of BMPs and prevented the progression of cartilage-subchondral bone lesions in rat knees with a DMM. Selective exercise timing may be a key factor in the development of an exercise regimen for preventing the progression of post-traumatic osteoarthritis (PTOA). Furthermore, exercise may have favorable effects even after the PTOA has been developed.

© 2016 Osteoarthritis Research Society International. Published by Elsevier Ltd. All rights reserved.

Introduction

Post-traumatic osteoarthritis (PTOA) is a common chronic joint disease, causing approximately 10% of the overall prevalence of

* Address correspondence and reprint requests to: H. Kuroki, 53 Shogoin, Kawahara-cho, Sakyo-ku, Kyoto 606-8507, Japan. Tel: 81-75-751-3963; fax: 81-75-751-3909.

E-mail addresses: iijima.hirota.75s@st.kyoto-u.ac.jp (H. Iijima), aoyama.tomoki.4e@kyoto-u.ac.jp (T. Aoyama), legacy-ts.akira_ito@live.jp (A. Ito), junichi_tajino@icloud.com (J. Tajino), yamaguchi.shouki.26n@st.kyoto-u.ac.jp (S. Yamaguchi), nagai@cac.med.kyoto-u.ac.jp (M. Nagai), kiyan.wataru.32c@st.kyoto-u.ac.jp (W. Kiyon), zhang.xiangkai.48v@st.kyoto-u.ac.jp (X. Zhang), kuroki.hiroshi.6s@kyoto-u.ac.jp (H. Kuroki).

symptomatic knee OA¹. Effective viable treatments for PTOA are required to reduce financial burden, but there is currently a lack of effective disease-modifying therapies. Although OA was historically considered to be primarily a disease of the articular cartilage, it is now considered to be a whole-joint disease typically accompanied by subchondral bone lesions². Accumulated evidence shows that there is cellular interaction and molecular crosstalk between articular cartilage and cortical subchondral bone^{3–5}, which may accelerate the progression of PTOA. A recent study revealed that the treatment that suppressed abnormal subchondral bone remodeling prevented secondary cartilage degeneration in an experimental PTOA model⁶. Thus, development of better PTOA interventions that target the entire joint instead of a single tissue, including the cartilage-subchondral bone unit, is warranted.

Chondrocytes and bone cells (including osteoblasts, osteoclasts, and osteocytes) within the cartilage-subchondral bone unit sense and respond to mechanical stimuli in a magnitude-dependent manner⁷. Current understanding from *in vitro* studies is that physiological mechanical loading has anti-inflammatory effects that upregulate the chondrogenic and osteogenic activities of the joint cells^{7,8}, suggesting that exercise intervention may act as a disease-modifying therapy for PTOA. However, there is a lack of evidence of exercise efficacy on the cartilage-subchondral bone unit in PTOA knees *in vivo*. Based on these ideas, we recently demonstrated that moderate level treadmill exercise was effective in preventing osteoarthritic changes to the cartilage-subchondral bone unit in the rat model of destabilized medial meniscus (DMM) through 4 weeks after surgery⁹. The pathologic changes in the cartilage and subchondral bone alterations in this model are similar to the changes seen in human PTOA¹⁰. Because 4 weeks post-DMM would be still considered the transient period, further investigation into the effects of exercise targeting the cartilage-subchondral bone unit at later times, after PTOA has more developed, would be of interest.

Subjects in human OA clinical trials are likely to be at various stages of the disease when an exercise intervention is initiated¹¹. Conversely, exercise is often initiated in pre-clinical animal models shortly after the PTOA process begins^{12,13}. Given that there is phasic development of PTOA with early matrix remodeling and transcriptional activity in an experimental PTOA model¹⁴, the response to intervention for treating PTOA would depend on the timing of the intervention. Nam *et al.* showed that the extent of cartilage damage at the initiation of moderate level exercise determined its effectiveness by having different regulatory effects on pro-inflammatory gene networks or matrix synthesis in monoiodoacetate-induced arthritis¹⁵. However, whether selective initiation timing of moderate level exercise can more effectively prevent cartilage-subchondral bone unit osteoarthritic changes is still unknown.

The purpose of the current study was: (1) to examine the long-term effects of moderate level treadmill exercise during the development of PTOA on the cartilage-subchondral bone unit, and (2) to investigate how the timing of initiation of exercise affects the efficacy of the exercise on the cartilage-subchondral bone unit, in a DMM rat model. The general hypotheses were that treadmill exercise prevents the progression of cartilage-subchondral bone osteoarthritic changes, and that exercise started shortly after DMM induction can better prevent the osteoarthritic changes than that started after PTOA has developed.

Method

Animals and surgical induction of osteoarthritis

This study was approved by the animal research committee of Kyoto University (approval number: Med Kyo 15025) and conducted accordance with ARRIVE guideline¹⁶. Twelve-week-old male Wistar rats ($n = 37$; mean body weight: 272.1 g) were purchased and kept three or four to a plastic cage in a 12-h light/dark cycle at constant temperature on sawdust bedding. The animals could move freely in the cages and had free access to food and water. The pre-clinical model of DMM was performed as described previously under anesthesia induced with 0.85 ml/kg somnopen-tyl⁹. Briefly, the surgery involved an incision into the medial capsule and transection of the anterior medial meniscotibial ligament (MMTL) on the right knee. A sham operation was performed on the left knee joint as an internal control using the same approach, but without transecting the MMTL.

Gentle treadmill walking (TW) regimens

The animals were randomly assigned to the sedentary ($n = 10$) or walking ($n = 27$) groups post-surgery to avoid any influence from the date when the surgery was performed. To prevent the animals from becoming differentially stressed, treadmill performance on a 1–5 Likert scale¹⁷ was evaluated in each animal in the walking group, as described previously⁹. Three of the 27 rats in the walking group were excluded because they displayed insufficient Likert scores, leaving 24 rats in the walking group. As described in Fig. 1, animals in the walking group were randomly assigned to the DMM + TW0–8, DMM + TW0–4, and DMM + TW4–8 groups ($n = 8$ per group). Subsequently, the animals in each walking group were subjected to gentle TW on a motor driven treadmill (Natsume Seisakusho Co., Tokyo, Japan) at 12 m/min for 30 min/day, 5 days/week from day 2 through 8 weeks, day 2 through 4 weeks, or 4 weeks through 8 weeks, respectively (Fig. 1). This exercise regimen was based on a protocol from an earlier study¹⁵. Previously, we found no apparent cartilage degeneration on day 2, and close to grade 3–3.5 cartilage damage at 4 weeks⁹, using the Osteoarthritis Research Society International (OARSI) scoring system established by Pritzker *et al.*¹⁸; to investigate the effects of exercise on already degenerated cartilage, TW in the DMM + TW4–8 group was started 4 weeks after DMM surgery. The animals in the sedentary group were allowed to move freely in standard cages without any TW for 8 weeks. All rats were euthanized 8 weeks after surgery.

Micro-computed tomography (micro-CT) analysis of subchondral bone changes

Before histological sectioning, all rat knee joints were scanned using a micro-CT system (SMX-100CT, Shimadzu, Kyoto, Japan) at voxel size 21 μm resolution. The reconstructed data sets were examined using three-dimensional data analysis software (Amira5.4, Visage, Berlin, Germany). The details of the scanning protocol and data analysis were recently described⁹. Briefly, we evaluated the subchondral bone plate thickness (Sb thickness) in the weight-bearing region of the medial tibia, defined as a region in the frontal plane of 0.5 mm mediolateral width and 1 mm ventrodorsal length. Additionally, the diameter of maximum subchondral bone cyst (SBC), defined as a tunnel-like corridor connecting the cartilage and subchondral bone marrow, and average diameter of three SBCs were measured in each DMM knee to allow comparison between groups. To analyze the proximal tibia, the following trabecular bone parameters in the epiphysis distal to the growth plate were evaluated: the trabecular bone volume fraction (Trab BV/TV), trabecular bone thickness (Tb.Th), and trabecular spacing (Tb.Sp)⁹. To determine whether the Trab BV/TV changed locally after DMM induction^{9,19}, the subchondral trabecular bone volume fraction (Sb BV/TV) was assessed in the epiphysis proximal to the medial subchondral bone plate.

Histological preparation and semi-quantitative analysis of osteoarthritis severity

Decalcified paraffin sections were prepared from the rat knee joints in the frontal plane according to the OARSI recommendations described by Gerwin *et al.*²⁰. Three 6 μm paraffin sections spaced at 200 μm intervals spanning each entire knee joint were stained with toluidine blue to evaluate the severity of cartilage lesions, and hematoxylin–eosin to determine the severity of the subchondral bone lesions. The OARSI scoring system, consisting of six grades and four stages on a scale from 0 (normal) to 24 (severe cartilage lesion)¹⁸, was used for semi-quantitative evaluation of cartilage lesion severity. The most severe score among the three sections was

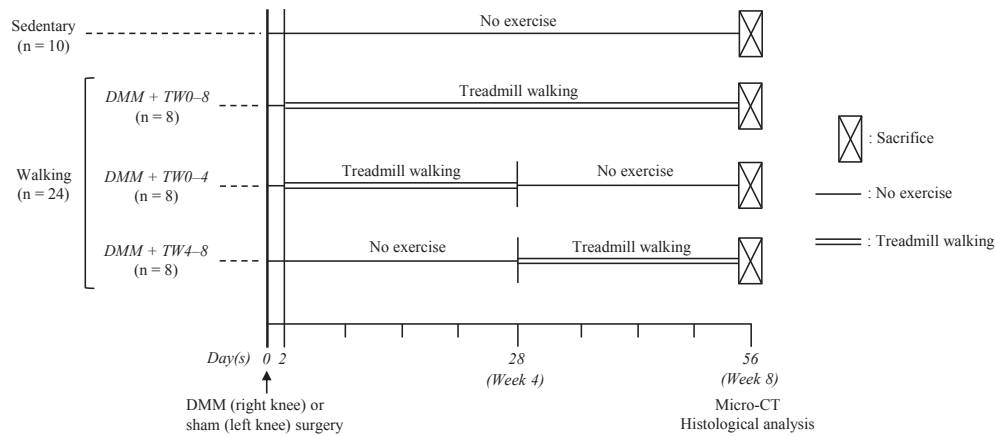


Fig. 1. Experimental protocols. All rats underwent DMM surgery on their right knee and sham surgery on their left knee and were assigned to either the sedentary group ($n = 10$) or the walking group ($n = 24$). The rats in the walking group were randomly assigned to the DMM + TW0-8, DMM + TW0-4, and DMM + TW4-8 groups ($n = 8$ per group). The rats in each walking group were subjected to TW (12 m/min, 30 min/day, 5 days/week) from day 2 through 8 weeks, day 2 through 4 weeks, or 4 weeks through 8 weeks, respectively. At 8 weeks after DMM induction, the rats were euthanized and assessed with micro-CT and histological analyses.

defined as the maximum OARSI score, and the summed total of the three highest section scores was also determined and defined as the summed OARSI score. These summed scores provide a measure of the “extent” of the cartilage lesions, as a representation of their relative volume, in the medial tibia.

Next, we evaluated the calcified cartilage and subchondral bone damage score (SB damage score) on a scale from 0 (normal) to 5 (severe subchondral bone lesions) to assess the severity of subchondral bone lesions, as described previously²⁰. As was done for the OARSI score, we calculated the maximum SB damage score and the summed SB damage score. The OARSI and SB damage scores were evaluated by a single trained observer (HI), and the intrarater reliability scores were excellent for both the OARSI and the SB damage scores (intraclass correlation coefficient: 0.92 and 0.97, respectively).

The number of empty osteocyte lacunae per square millimeter and the total number of lacunae per square millimeter, the lacunae density, in the subchondral bone surface were also calculated. Data analysis methods were slightly modified from those described recently⁹. Here, we measured the empty osteocyte lacunae and lacunae density within standardized rectangular fields (100 μm deep by 500 μm long) in the subchondral bone underneath the calcified cartilage in the medial tibia.

Histochemical and immunohistochemical analyses

Osteoclasts and osteoblasts were visualized by histochemical staining for tartrate-resistant acid phosphatase (TRAP) and alkaline phosphatase (ALP) activities using the TRAP/ALP stain kit (Wako, Osaka, Japan) according to manufacturer instructions. The distribution of TRAP- and ALP-positive cells in the subchondral bone was qualitatively evaluated. Additionally, immunohistochemistry was performed to determine the tissue distribution of type II collagen, bone morphogenetic protein-2 (BMP-2) and BMP-6. The antigen retrieval and blocking steps were performed essentially as previously described²¹. Sections were then incubated with anti-type II collagen (diluted 1:200; Fine Chemical Co., Toyama, Japan), anti-BMP-2 (diluted 1:100; Abcam Co., Tokyo, Japan), or anti-BMP-6 (diluted 1:200; Abcam) primary antibodies. Detection was performed using the streptavidin–biotin–peroxidase complex technique with an Elite ABC kit, and immunoreactivity was visualized by incubation with diaminobenzidine solution (Vector Laboratories, Burlingame, CA, USA) followed by counterstaining with hematoxylin. The primary antibody was omitted from the negative control slides. The expression of type II collagen in the medial tibial cartilage was semi-

quantitatively analyzed by measuring the pixel intensity values in the matrix staining on a scale from 0 to 255 (0 = no staining; 255 = maximum staining), using ImageJ software and methods slightly modified from those described previously²². Additionally, the expression of BMP-2 and BMP-6 in the chondrocytes was defined as the percentage of BMP-2- and BMP-6-positive chondrocytes within the middle region of the medial tibia with a mediolateral width of 0.5 mm. The percentage of BMP-2- and BMP-6-positive bone-lining cells, including osteoblasts, was also evaluated from standardized rectangular fields (500 μm deep and 500 μm long, excluding SBC area) within the subchondral bone of the middle region in the medial tibia.

Statistical analysis

Statistical analyses were performed using the JMP 11 software program (SAS Institute, Cary, NC, USA), and data from the following five groups were analyzed; the DMM-operated knee of the sedentary group (DMM group) and the three walking groups (DMM + TW0-8, DMM + TW0-4, and DMM + TW4-8 groups), and the sham operated knee of the sedentary group (sham group). The data are displayed as means with uncertainty expressed as 95% confidence intervals (mean \pm 95% CI) for continuous data, and as medians and ranges (median [lower range–upper range]) for categorical data. All continuous data were assessed for Gaussian distribution using the Shapiro–Wilk normality test, and for homoscedasticity using Bartlett’s test. The differences among the groups, considering the multiple testing error, were evaluated using analysis of variance, and *post hoc* Tukey–Kramer tests were used subsequently for parametric continuous data. The Kruskal–Wallis tests and subsequently, *post hoc* Steel–Dwass tests were used for nonparametric continuous data or categorical data. In all experiments, P -values < 0.05 were considered statistically significant. Throughout this text, “ n ” represents the number of independent observations from different animals per group.

Results

Gentle TW prevented the progression of articular cartilage lesions and increased the expression of BMPs in superficial zone chondrocytes

As shown in Fig. 2(A), the medial tibial cartilage in the DMM group showed a severe proteoglycan loss, loss of the superficial zone, and decrease in the number of chondrocytes. However, the

cartilage in the three walking groups had a smooth surface with viable superficial zone chondrocytes, particularly in the *DMM + TW4–8* group, which was evidenced by a significantly lower OARSI score in this group than that in the *DMM* group, in both the maximum (5 [2–9] vs 12 [6–16.5]) and summed (10 [6–21] vs 27 [18–42]) scores [Fig. 2(B)]. The expression of type II collagen in the cartilage in the *DMM* group exhibited a 25% lower staining intensity than that in the *sham* group ($P = 0.002$), but there were no significant differences between the *DMM* group and the three walking groups [Fig. 2(C)].

Next, we investigated whether TW increased BMP-2 and -6 expressions in the chondrocytes (Fig. 3). Moderate biomechanical stimuli have been shown to induce BMP-2 and -6 expressions in the chondrocytes⁸, increasing proteoglycan and type II collagen synthesis^{23,24}. The results showed weak but widely BMP-2-positive chondrocytes in the *sham* group [Fig. 3(A)]. However, in the degenerated cartilage in the *DMM* group, there was a decrease in BMP-2-positive chondrocytes. TW mitigated this loss of BMP-2-positive chondrocytes to a varying extent depending on the

walking conditions. As shown in Fig. 3(B), only the cartilage in the *DMM + TW4–8* group showed a significantly higher percentage of BMP-2-positive chondrocytes than that in the *DMM* group ($30.3 \pm 5.9\%$ vs $18.3 \pm 5.2\%$). Although, the percentages of BMP-2-positive chondrocytes in the *DMM* and the three walking groups were lower than those in the *sham* group ($43.8 \pm 5.9\%$), more abundant and intense BMP-2 staining was found around the degenerated cartilage in those groups compared to the normal cartilage in the *sham* group.

In contrast to the BMP-2 staining pattern, the cartilage in the *sham* group exhibited almost no BMP-6-positive ($0.1 \pm 0.2\%$) chondrocytes [Fig. 3(C)]. Interestingly, most superficial zone chondrocytes demonstrated BMP-6 expression in response to TW, a slightly different pattern than that of the BMP-2 expression, whereas chondrocytes in the *DMM* group exhibited only weak BMP-6-positive superficial zone staining. The cartilage in the *DMM + TW4–8* group had a significantly higher percentage of BMP-6-positive chondrocytes ($27.3 \pm 6.5\%$) than that in the *DMM* ($12.9 \pm 3.0\%$) and *DMM + TW0–4* ($15.2 \pm 5.0\%$) groups.

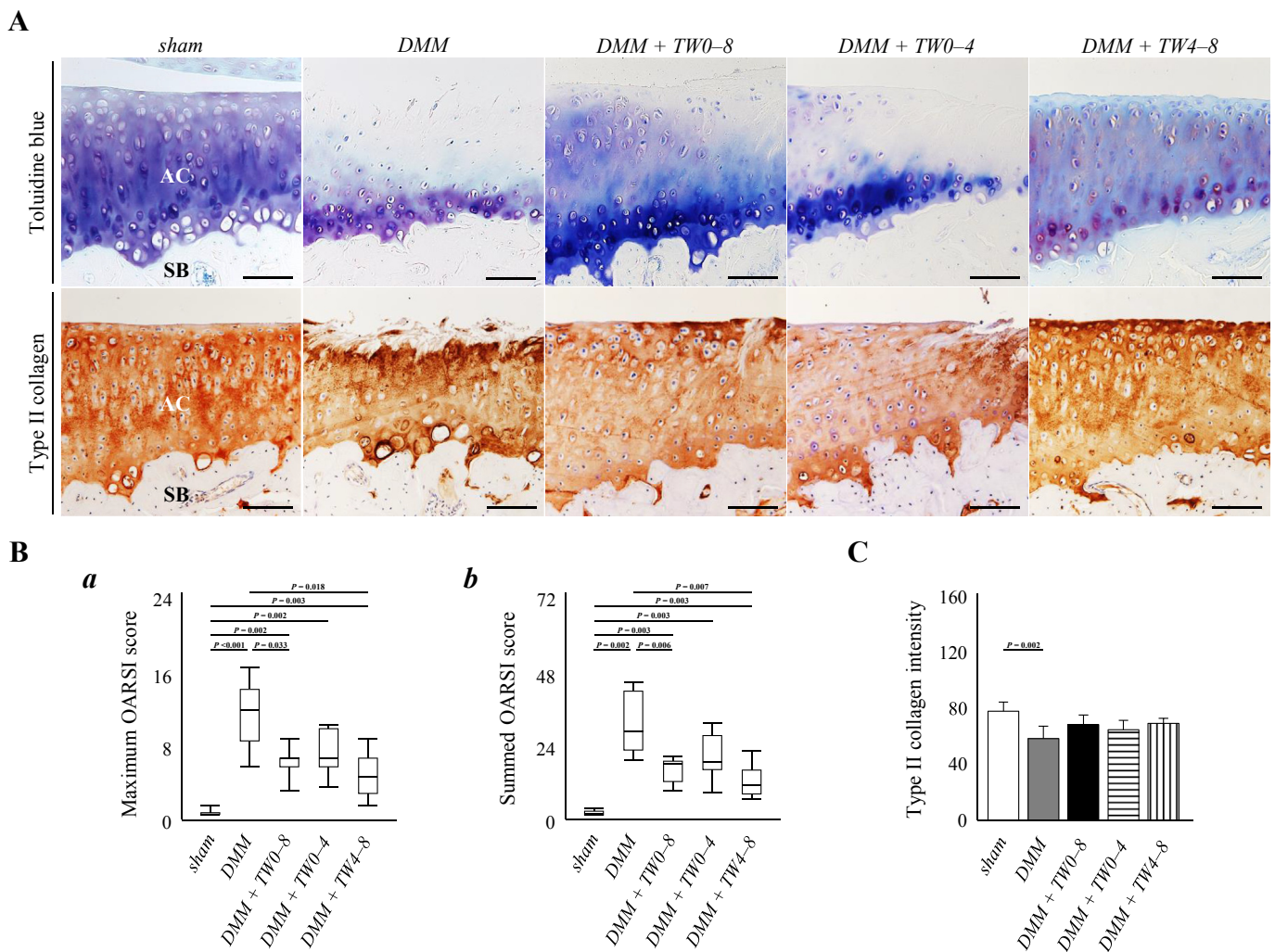


Fig. 2. TW prevented the development of articular cartilage lesions induced by the *DMM*. **A**, Histological images of toluidine blue- and type II collagen-stained sections of the medial tibia at 8 weeks after surgery. Magnification: $\times 200$. Scale bars = 100 μm . AC: articular cartilage; SB: subchondral bone. **B**, Semi-quantitative analysis of the cartilage lesions in the medial tibia using the OARSI scoring system at 8 weeks after surgery. The maximum OARSI score (a), the most severe score among all three evaluated histological sections, and the summed OARSI score (b), the summed total score of all three evaluated histological sections. Boxplots display the medians and interquartile ranges, and vertical bars display the ranges of the independent experiment ($n = 10$ for the *sham* and *DMM* groups, and $n = 8$ for the *DMM + TW0–8*, *DMM + TW0–4*, and *DMM + TW4–8* groups). P -value was calculated using the Steel–Dwass test as *post hoc* analysis of the Kruskal–Wallis test. **C**, Type II collagen pixel intensity (range: 0–255, with 0 indicating no staining and 255 indicating maximum staining) in the medial tibia at 8 weeks after surgery. Values are the means \pm 95% CI of the independent experiment ($n = 10$ for the *sham* and *DMM* groups, and $n = 8$ for the *DMM + TW0–8*, *DMM + TW0–4*, and *DMM + TW4–8* groups). P -value was calculated using the Tukey–Kramer test as *post hoc* analysis of the analysis of variance.

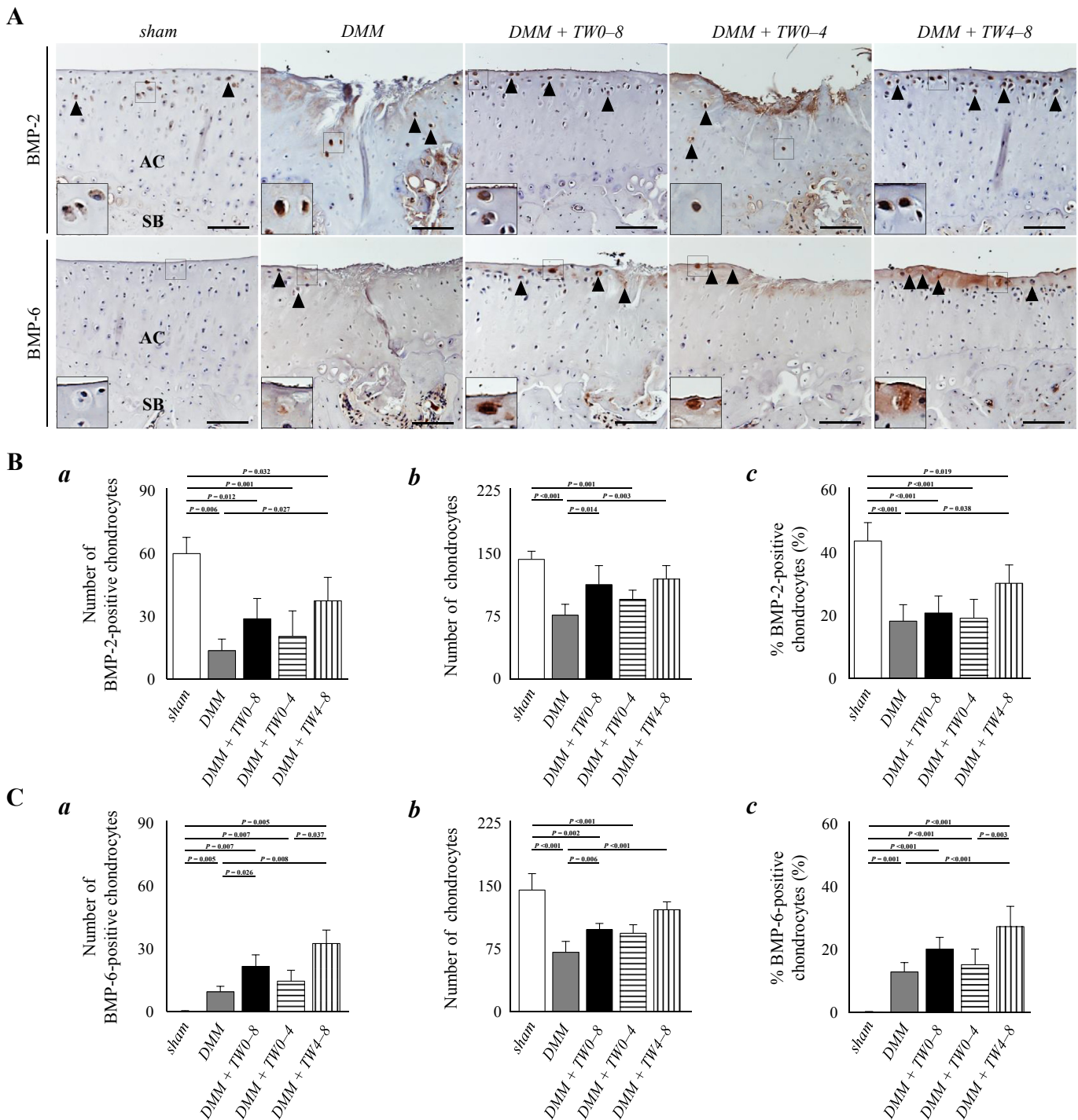


Fig. 3. TW regulated the secretion of BMPs by superficial zone chondrocytes. **A**, Representative medial tibial cartilage sections stained for BMP-2 and BMP-6 at 8 weeks after surgery. Black arrow head indicates representative BMP-2- and BMP-6-positive chondrocytes. Magnification: $\times 200$. Insets: Higher magnification views ($\times 500$) of the boxed areas within the same image. Scale bars = 100 μm . AC: articular cartilage; SB: subchondral bone. **B, C**, Quantitative analysis of BMP-2 (**B**) and BMP-6 (**C**) secretion by chondrocyte. (a) Number of BMP-2- and BMP-6-positive chondrocytes, (b) the number of chondrocytes, and (c) the percentage of BMP-2- and BMP-6-positive chondrocytes, which is the number of BMP-2- and BMP-6-positive chondrocytes divided by the number of chondrocytes within an area with a mediolateral width of 0.5 mm in the middle region of the medial tibia respectively. Values are the means \pm 95% CI of the independent experiment ($n = 10$ for the sham and DMM groups, and $n = 8$ for the DMM + TW0-8, DMM + TW0-4, and DMM + TW4-8 groups). *P*-value was calculated using the Steel–Dwass test as *post hoc* analysis of the Kruskal–Wallis test (for the number of BMP-2- and BMP-6-positive chondrocytes [a]) and Tukey–Kramer test as *post hoc* analysis of the analysis of variance (for the number of chondrocytes [b] and the percentage of BMP-2- and BMP-6-positive chondrocytes [c]).

Gentle TW suppressed the increase in localized subchondral bone lesions and improved osteocyte viability

The micro-CT analyses showed that the DMM-induced localized subchondral bone perforations in the medial tibial plateau, which

were partially prevented by TW [Fig. 4(A)]. The measured maximum and averaged SBC diameters on the frontal plane images [Fig. 4(B)] showed suppression of SBC growth with TW; the DMM + TW4-8 group showed the most effective suppression of SBC growth and significantly lower maximum and average SBC

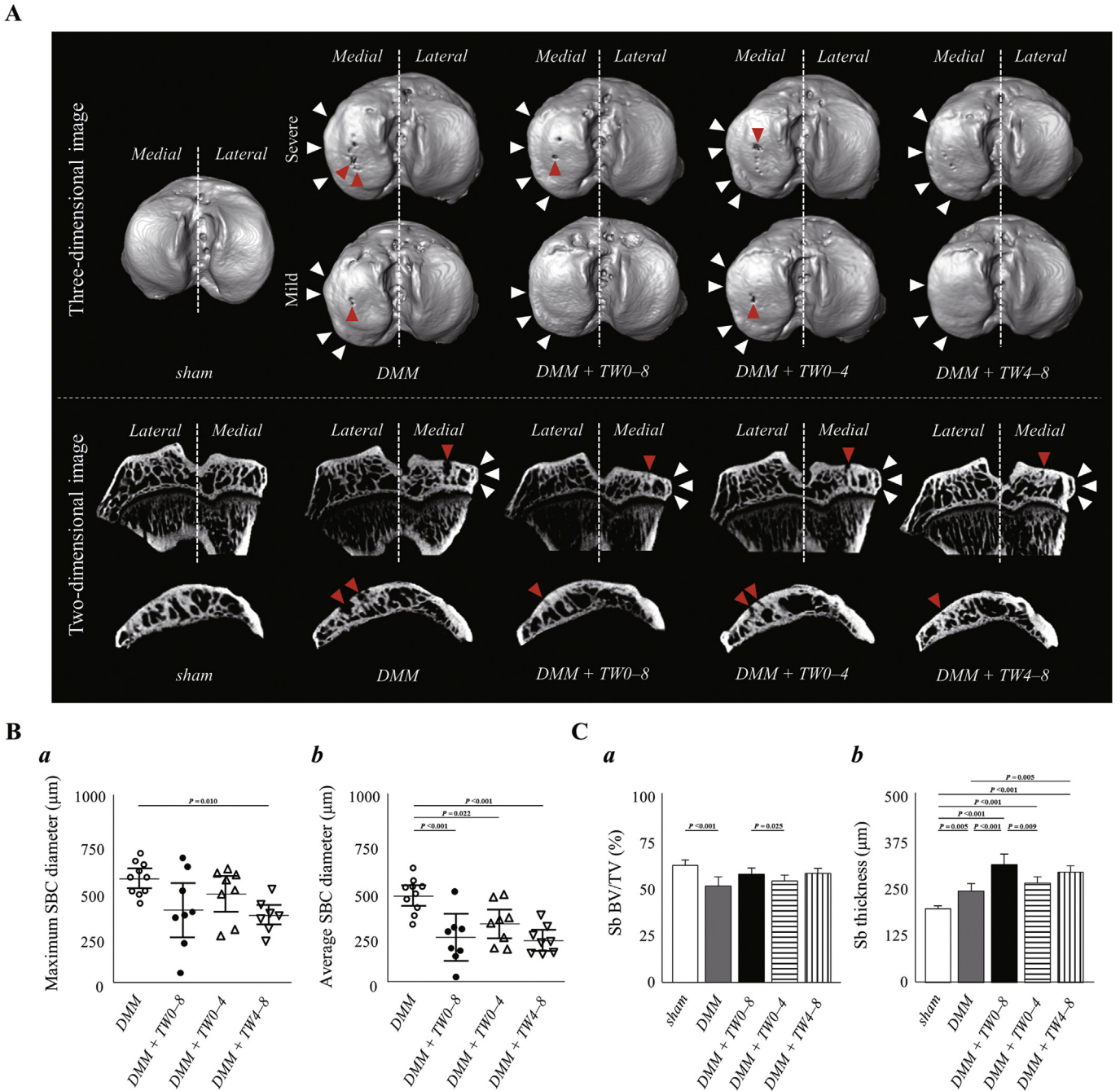


Fig. 4. DMM-induced localized subchondral bone porosity in the medial tibial plateau that was prevented by TW. **A**, Representative three-dimensional and two-dimensional micro-CT images of the subchondral bone in severe and mild osteoarthritic knees. Subchondral bone perforations (red arrow head) were found in the medial tibial plateau on the three-dimensional surface views, particularly in the DMM group. The two-dimensional images of the knee joints show the presence of SBCs in the medial tibia (red arrow head) that correspond to the region of the bone perforations found in the three-dimensional surface view. Osteophyte mineralization was confirmed at the medial margin with some inter-individual variability in all samples of the DMM and the three walking groups (white arrow head). **B**, Measurement of SBC diameters. (a) The maximum SBC diameter, and (b) the average of three SBC diameters. Horizontal bars display the means, and vertical bars display the 95% CI of the independent experiment ($n = 10$ for the DMM group, and $n = 8$ for the DMM + TW0-8, DMM + TW0-4, and DMM + TW4-8 groups). P -value was calculated using the Tukey–Kramer test as *post hoc* analysis of the analysis of variance. **C**, Quantitative analysis of the subchondral bone parameters. (a) The bone volume/total volume of subchondral bone underneath the subchondral bone plate (Sb BV/TV) and (b) Sb thickness in the medial tibia. Values are the means \pm 95% CI of the independent experiment ($n = 10$ for the sham and DMM groups, and $n = 8$ for the DMM + TW0-8, DMM + TW0-4, and DMM + TW4-8 groups). P -value was calculated using the Tukey–Kramer test as *post hoc* analysis of the analysis of variance.

diameters than the DMM group (maximum: $361.1 \pm 68.5 \mu\text{m}$ vs $586.0 \pm 55.6 \mu\text{m}$; average: $256.1 \pm 50.9 \mu\text{m}$ vs $495.6 \pm 56.0 \mu\text{m}$). Furthermore, TW, particularly in the DMM + TW0-8 and the DMM + TW4-8 groups, mitigated the DMM-induced decrease in the Sb BV/TV, resulting in a thick subchondral bone plate [Fig. 4(C)]. However, neither DMM surgery nor TW markedly affected the

trabecular bone parameters distal to the growth plate (Supplementary Fig. 1).

Based on the micro-CT data, we histologically examined the subchondral bone, focusing on the medial tibia (Fig. 5). TW prevented the progression of subchondral bone lesions, including bone collapse, and suppressed the increase in osteocyte death induced by the DMM

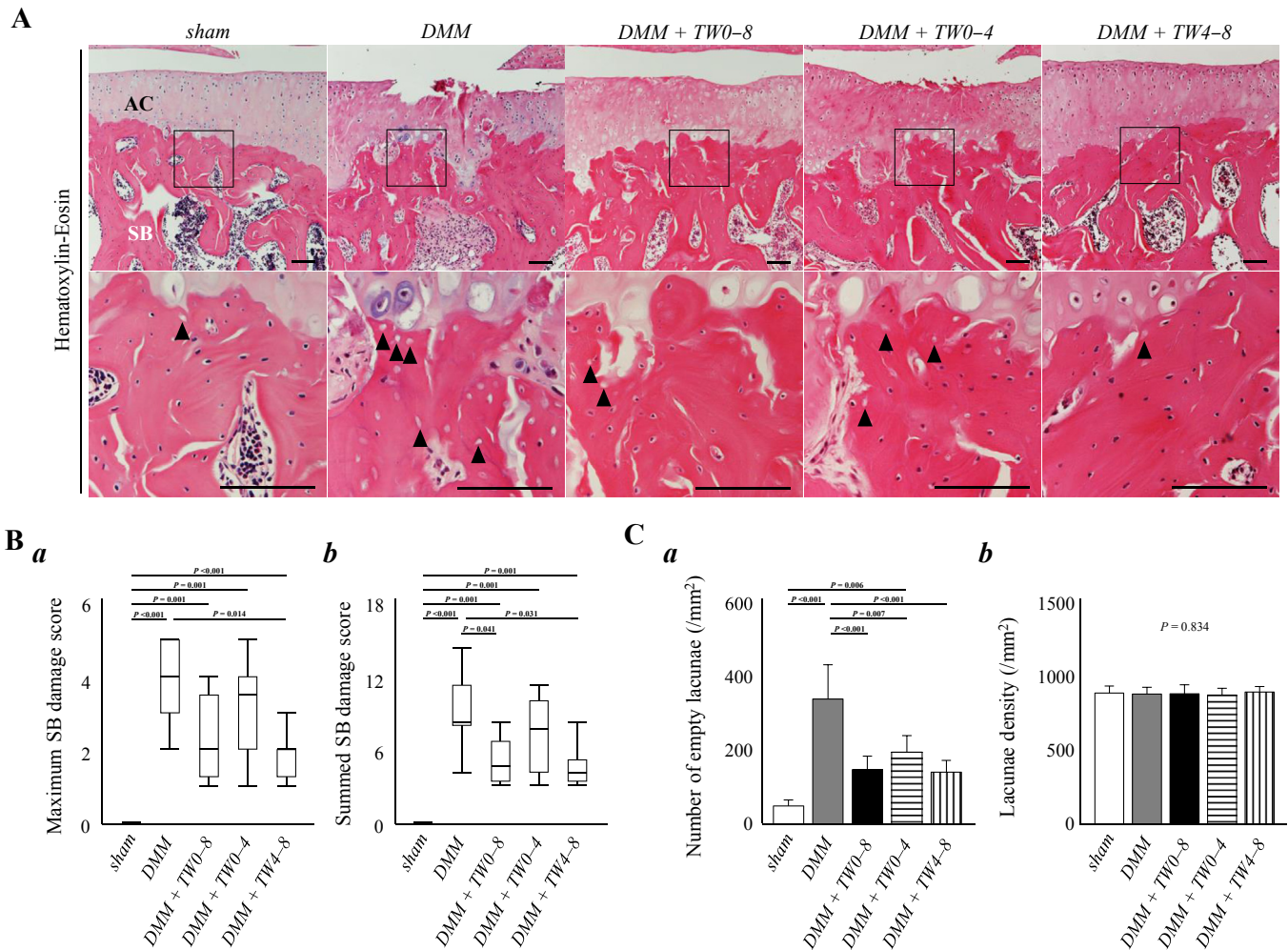


Fig. 5. TW prevented the progression of subchondral bone lesions and suppressed the increase in osteocyte death induced by the DMM. **A**, Histological images of hematoxylin–eosin-stained sections of the medial tibia. Magnification: $\times 100$. Scale bars = 100 μm . AC: articular cartilage; SB: subchondral bone. Empty osteocyte lacunae was confirmed in the subchondral bone underneath the degenerated cartilage (black arrow head), particularly in the DMM group. The black box is a magnification ($\times 400$) of the figure below. **B**, Semi-quantitative assessment of the subchondral bone lesions in the medial tibia using the calcified cartilage and SB damage scores. (a) The maximum SB damage and (b) the summed SB damage scores. Boxplots display the medians and interquartile ranges, and vertical bars display the ranges of the independent experiment ($n = 10$ for the sham and DMM groups, and $n = 8$ for the DMM + TW0–8, DMM + TW0–4, and DMM + TW4–8 groups). *P*-value was calculated using the Steel–Dwass test as *post hoc* analysis of the Kruskal–Wallis test. **C**, Effects of TW on (a) the number of empty osteocyte lacunae ($/\text{mm}^2$) and (b) the lacunae density ($/\text{mm}^2$), which includes both the number of empty and healthy osteocyte lacunae. Values are the means \pm 95% CI of the independent experiment ($n = 10$ for the sham and DMM groups, and $n = 8$ for the DMM + TW0–8, DMM + TW0–4, and DMM + TW4–8 groups). *P*-value was calculated using the Steel–Dwass test as *post hoc* analysis of the Kruskal–Wallis test (for the number of empty osteocyte lacunae [a]) and analysis of variance (for the lacunae density [b]). Significantly different values ($P < 0.05$) are displayed in bold.

[Fig. 5(A)]. As shown in Fig. 5(B and C), among the three walking groups, the DMM + TW4–8 group showed the lowest SB damage scores (maximum: 2 [1–3]; summed: 4 [3–8]) and number of empty lacunae ($141.7 \pm 31.8 /\text{mm}^2$), which were significantly lower than those in the DMM group (SB damage score, maximum: 4 [2–5]; summed: 8 [4–14]; empty lacunae: $340.7 \pm 93.5 /\text{mm}^2$).

Gentle TW modulated osteogenic activity in the bone-lining cells

In the DMM group, abnormal bone remodeling, as shown by increased TRAP- and ALP-positive cells including osteoclasts and osteoblasts in the fibrous marrow space, was found in the area of the SBC identified by micro-CT [Fig. 6(A)]. The subchondral bone in the three walking groups exhibited a decreased number of TRAP-positive cells compared to the DMM group, and an increased number of ALP-positive bone-lining cells, including osteoblasts, particularly in the DMM + TW0–8 and DMM + TW4–8 groups.

We next examined the expression of BMP-2 and -6, which are secreted in response to moderate biomechanical stimuli⁸ and

strongly accelerate osteogenesis²⁵. Bone-lining cells including osteoblasts in the DMM + TW0–8 and the DMM + TW4–8 groups, demonstrated a strong expression of BMP-2 and -6 [Fig. 6(A)]. The percentages of BMP-2- and -6-positive bone-lining cells [Fig. 6(B and C)] in the DMM + TW4–8 group were significantly higher than those in the DMM group (BMP-2: $85.6 \pm 4.4\%$ vs $74.8 \pm 2.9\%$; BMP-6: $86.2 \pm 2.1\%$ vs $76.0 \pm 4.5\%$). However, the percentages of BMP-2- and -6-positive osteocytes were very low ($<4\%$) and not significantly different between the groups (data not shown). In addition, the expression of BMPs in the osteophyte area was not markedly changed in response to TW, and the osteophyte volumes assessed by micro-CT were not significantly different between the groups (Supplementary Fig. 2).

Discussion

In the current study, we demonstrated that TW prevented the progression of both articular cartilage and subchondral bone lesions during the development of PTOA, even after PTOA has been

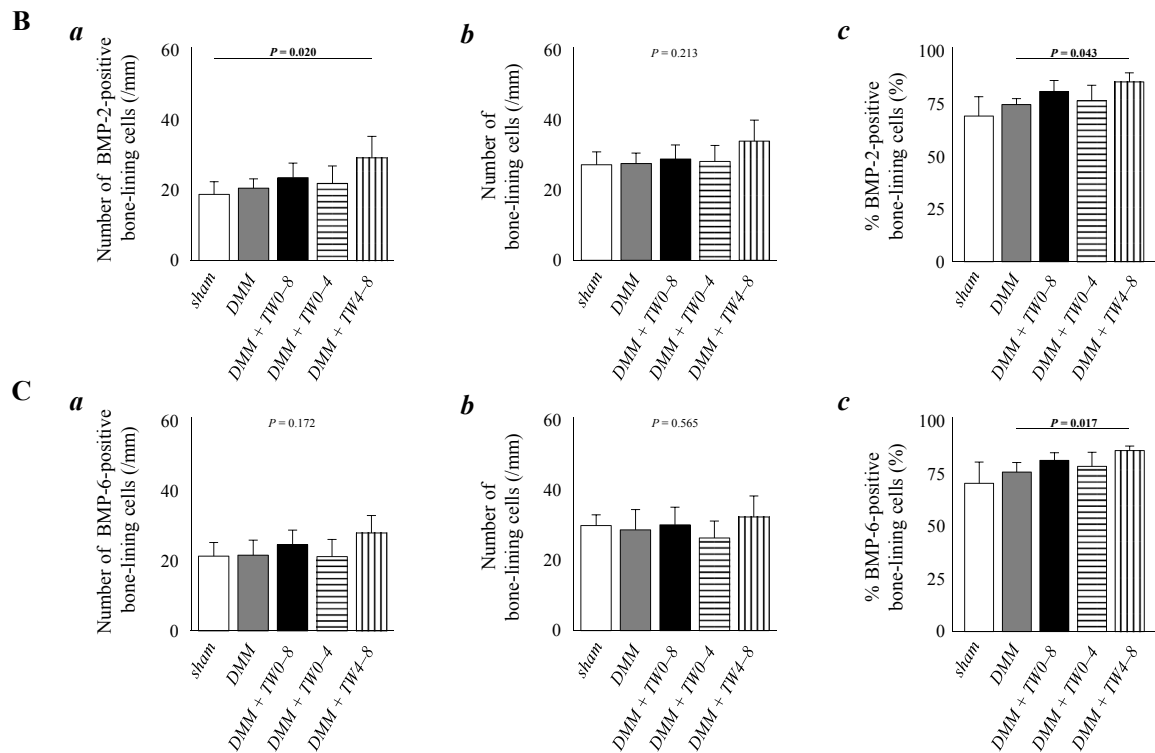
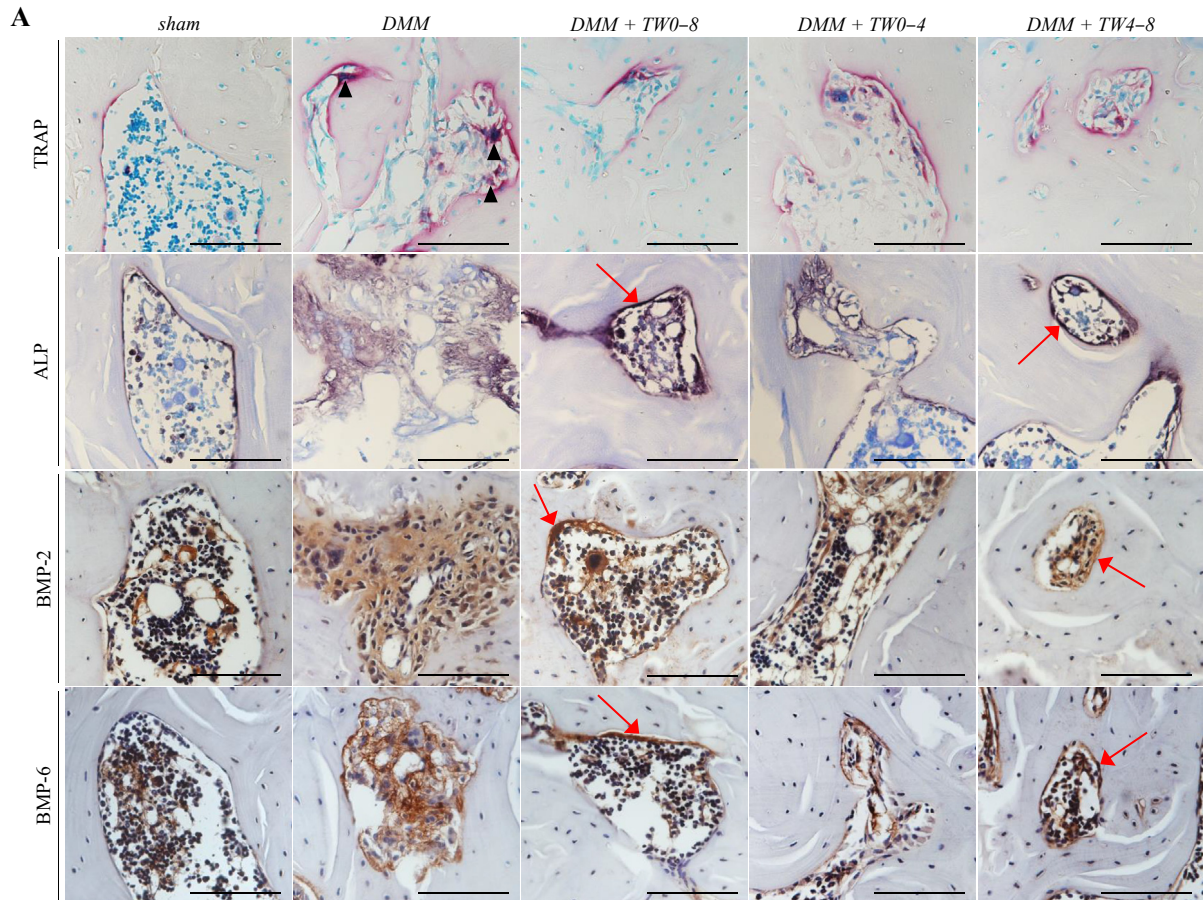


Fig. 6. TW modulated the activity of the cells that regulate subchondral bone remodeling in DMM knees. **A**, Representative images show the abnormal bone remodeling in the DMM group with an increased number of TRAP-positive osteoclasts (black arrow head) in the marrow space filled with fibrous tissue and an increase in the ALP, BMP-2, and BMP-6 staining in the bone-lining cells in response to TW (red arrow), particularly in the DMM + TW0-8 and the DMM + TW0-4 groups. Magnification: $\times 400$. Scale bars = 100 μm . **B**, **C**, Quantitative analysis of BMP-2 and BMP-6 secretion by bone-lining cells including osteoblasts. (a) Number of BMP-2- and BMP-6-positive bone-lining cells per bone surface (/mm), (b) the number of bone-lining cells per bone surface (/mm), and (c) the percentage of BMP-2- and BMP-6-positive bone-lining cells, which is the number of BMP-2- and BMP-6-positive bone-lining cells divided by the number of bone-lining cells. Values are the means \pm 95% CI of the independent experiment ($n = 10$ for the sham and DMM groups, and $n = 8$ for the DMM + TW0-8, DMM + TW0-4, and DMM + TW4-8 groups). P -value was calculated using the Tukey-Kramer test as *post hoc* analysis of the analysis of variance (for the number of BMP-2- and BMP-6-positive bone-lining cells [a] and the number of bone-lining cells [b]) and Steel-Dwass test as *post hoc* analysis of the Kruskal-Wallis test (for the percentage of BMP-2- and BMP-6-positive bone-lining cells [c]). Significantly different values ($P < 0.05$) are displayed in bold.

developed. Furthermore, we found that TW regulates BMP-2 and -6 secretions by superficial zone chondrocytes and bone-lining cells, which coincided with the prevention of osteoarthritic changes. DMM has been known to elevate capacity for crosstalk between cartilage and subchondral bone, which might lead progression of PTOA⁴. Specifically, local factors secreted by human sclerotic osteoblasts contribute to downregulation of aggrecan and upregulation of matrix metalloproteinases-3 and -13 by human chondrocytes⁵. Conversely, treatment that targets a single tissue might lead to improvement in the other tissue²⁶. Recently, Nam *et al.* showed that physiological biomechanical stimulation for osteoblast regulated gene expression by chondrocyte *via* paracrine manner⁸. Additionally, given that TW prevented SBC growth that are also cause of elevated crosstalk between cartilage and subchondral bone, beneficial effects of TW might include the modifying cellular and molecular interaction between cartilage and subchondral bone.

We demonstrated that the most effective TW regimen was started 4 weeks post-DMM. These results are unexpected and show opposite trends than those in a previous study that showed exercise intervention at the early stages of cartilage damage provided greater benefits in monoiodoacetate-induced arthritis¹⁵. In that model, acute inflammation induces rapid chondrocyte death, cartilage matrix loss, and osteoclast activation in the across the joint surface, including both the medial and lateral compartments^{27,28}. In contrast, the DMM model induces mild focal cartilage and subchondral bone damage that is restricted to the medial compartment^{9,21}. Although both models are used as representative of PTOA, the DMM model shows a different time course for degenerative changes than the monoiodoacetate model¹⁰. Loeser *et al.* reported that the early phases at 2 and 4 weeks after DMM induction were the most active in terms of matrix remodeling gene expression¹⁴. Given that the level of inflammation present in the joint possibly affects the biological response of cartilage to mechanical load²⁹, these phasic development of DMM-induced PTOA may be related to the response of chondrocytes and bone cells to exercise in an attempt to delay the progression of PTOA.

We quantified the size of osteophytes and demonstrated no significant size difference among the experimental conditions, in which the BMP-2-positive osteophyte chondrocytes appear equal (Supplementary Fig. 2). This finding might indicate that the preventive effects of exercise intervention on cartilage-subchondral bone lesions might be independent of osteophyte growth. Nevertheless, the shape of the osteophyte probably affects the loading characteristics more compared to the size of the osteophyte. It is well-known that osteophyte formation is highly linked to changes of loading environment in the knee joint, and osteophytes stabilize anterior–posterior or varus–valgus laxities in the knee joint^{30,31}, which are associated with progression of PTOA³². Previously, we confirmed osteophyte formation in the knee joint 4 weeks after DMM induction²¹. These early bone adaptations in a DMM knee might explain why the late TW that was initiated 4 weeks after surgery was more effective in this study; the already created osteophytes re-distribute mechanical loading and stabilize the DMM-operated knee joint, which might enhance the effectiveness of the TW in the prevention of PTOA progression.

We first found that TW promoted BMP secretions by superficial zone chondrocytes as well as bone-lining cells. Our finding supports a previous *in vitro* study that showed that physiological biomechanical stimulation upregulated BMP synthesis of chondrocytes and osteoblasts within osteochondral constructs⁸. Currently, locally produced BMPs have been known to contribute to the intrinsic repair capacity of damaged cartilage and enhance cartilage repair²⁴ after traumatic injury or in osteoarthritic cartilage^{33,34}. Importantly, BMP-2 and -6 induce chondrogenesis in stem cells and enhance cartilage matrix synthesis *in vivo*^{23,24,35–37}, and

there is some *in vitro* evidence for an antagonistic activity of BMPs on the effects of interleukin-1³⁸. Similar to their cartilage effects, BMP-2 and -6 can enhance bone regeneration *in vivo*²⁵. In particular, BMP-6 strongly promotes osteoblast differentiation and bone formation^{39,40}. There may be synergistic effects of the combination of BMP-2 and -6, although such synergy has only so far been examined in BMP-2 and -7⁴¹. Although our findings were exploratory and hypothesis generating rather than conclusive, we suppose that an increased secretion of BMP-2 and -6 in response to TW may indicate an enhanced tissue-specific intrinsic repair capacity by chondrocytes and osteoblasts in the DMM knee. Exercise-elevated bone repair capacity might be supported by our findings that TW after DMM improved osteocyte viability, elevated osteoblastic activity, and thickened the subchondral bone plate (Figs. 4 and 6). Since osteocytes act as mechanosensors that modulate the activity of the main cell types regulating bone remodeling, TW might modify the activated bone-remodeling process that, in turn, thickens the subchondral bone plate. On a related note, there was no significant difference in the BMP-2 and -6 expressions in the osteocytes (data not shown), indicates that regulating the bone-remodeling process might include more than secretion of BMPs by osteocytes.

There are important limitations to the present study. Although the DMM model exhibits histologic features similar to those found in human PTOA¹⁰, this model is more severe than typical human PTOA. Additionally, immunostaining for BMP-2 was almost nonexistent in normal adult human articular cartilage⁴², whereas BMP-2-positive chondrocytes were even found in the cartilage of the sham knees in the present study; such differences should be considered when trying to translate our findings to human PTOA. Nevertheless, moderate levels of exercise may be beneficial for improving knee cartilage glycosaminoglycan content in middle-aged individual and patients at high risk of developing human OA^{11,43}. Since patients in human clinical trials will be at various disease stages when the intervention is initiated, our findings highlight that the timing of exercise initiation should be considered to develop better exercise regimens for treating human PTOA. Another important limitation is lack of variety in exercise intensity, although, we chose exercise protocol based on earlier study that showed anti-inflammatory/matrix synthesis effects of treadmill exercise in monoiodoacetate-induced arthritis¹⁵. As articular cartilage responds to mechanical stimuli with dose-dependent manner^{7,12,13,44}, investigating multiple intensity level exercise would be worth doing to elucidate whether these manners are confirmed even in cartilage-subchondral bone unit. Nevertheless, exercise protocol used in this study is consistent with previous studies that assessed chondroprotective effects for adult or instability-induced OA model rat knees (12–18 m/min for 30–60 min/day, 3–7 days/week)^{12,13,15,45}. Additionally, given that BMP-2 and -6 mRNA expressions were upregulated in cartilage and subchondral bone after 2 days of exercise with 12 m/min in adult rat⁸, exercise intensity used in this study would be sufficient to induce beneficial effects on DMM rat knees.

In conclusion, this study showed that long-term gentle TW prevents osteoarthritic changes in the cartilage-subchondral bone unit, which coincides with increased BMP-2 and -6 secretions by chondrocytes and bone-lining cells including osteoblasts. In addition, our results indicate that considering the timing of exercise initiation is one of the options for determining exercise efficacy and dynamically regulating BMP secretion. Furthermore, our data indicate that exercise intervention may have favorable effects even after PTOA has been developed. Further studies are needed to establish a basis for developing the more suitable intervention for preventing the progression of PTOA.

Author contributions

All authors have made substantial contributions to (1) the conception and design of the study, acquisition of data, or analysis and interpretation of data; (2) drafting the article or revising it critically for important intellectual content; and (3) final approval of the version to be submitted.

The specific contributions of the authors are as follows:

- (1) Conception and design of the study: HI, TA, AI, and SY.
- (2) Analysis and interpretation of the data: HI, TA, AI, SY, MN, XZ, WK, and HK.
- (3) Drafting of the article: HI, TA, AI, JT, SY, and HK.
- (4) Critical revision of the article for important intellectual content: HI, TA, AI, MN, WK, and HK.
- (5) Final approval of the article: HI and HK.
- (6) Statistical expertise: HI, TA, and JT.
- (7) Obtaining of funding: HI and HK.
- (8) Collection and assembly of data: HI and AI.

Role of the funding source

This study was supported in part by a Grant-in-Aid from the Japan Society for the Promotion of Science (<https://www.jsps.go.jp/>) Research Fellows (no. 270304) to HI, a JSPS KAKENHI Grant-in-Aid for Scientific Research (A) (no. 25242055), and a JSPS KAKENHI Grant-in-Aid for Challenging Exploratory Research (no. 25560258) to HK.

Conflict of interest

The authors have no relevant conflicts of interest to disclose.

Acknowledgments

The authors would like to thank Mr Takuya Isho (Rehabilitation Center, Fujioka General Hospital) for assistance in data analysis.

Supplementary data

Supplementary data related to this article can be found at <http://dx.doi.org/10.1016/j.joca.2016.01.006>.

References

1. Brown TD, Johnston RC, Saltzman CL, Marsh JL, Buckwalter JA. Posttraumatic osteoarthritis: a first estimate of incidence, prevalence, and burden of disease. *J Orthop Trauma* 2006;20:739–44.
2. Loeser RF, Goldring SR, Scanzello CR, Goldring MB. Osteoarthritis: a disease of the joint as an organ. *Arthritis Rheum* 2012;64:1697–707.
3. Lories RJ, Luyten FP. The bone-cartilage unit in osteoarthritis. *Nat Rev Rheumatol* 2011;7:43–9.
4. Pan J, Wang B, Li W, Zhou X, Scherr T, Yang Y, et al. Elevated cross-talk between subchondral bone and cartilage in osteoarthritic joints. *Bone* 2012;51:212–7.
5. Sanchez C, Deberg MA, Piccardi N, Msika P, Reginster JY, Henrotin YE. Osteoblasts from the sclerotic subchondral bone downregulate aggrecan but upregulate metalloproteinases expression by chondrocytes. This effect is mimicked by interleukin-6, -1beta and oncostatin M pre-treated non-sclerotic osteoblasts. *Osteoarthritis Cartilage* 2005;13:979–87.
6. Zhen G, Wen C, Jia X, Li Y, Crane JL, Mears SC, et al. Inhibition of TGF-beta signaling in mesenchymal stem cells of subchondral bone attenuates osteoarthritis. *Nat Med* 2013;19:704–12.
7. Nam J, Aguda BD, Rath B, Agarwal S. Biomechanical thresholds regulate inflammation through the NF-kappaB pathway: experiments and modeling. *PLoS One* 2009;4:e5262.
8. Nam J, Perera P, Rath B, Agarwal S. Dynamic regulation of bone morphogenetic proteins in engineered osteochondral constructs by biomechanical stimulation. *Tissue Eng Part A* 2013;19:783–92.
9. Iijima H, Aoyama T, Ito A, Yamaguchi S, Nagai M, Tajino J, et al. Effects of short-term gentle treadmill walking on subchondral bone in a rat model of instability-induced osteoarthritis. *Osteoarthritis Cartilage* 2015;23:1563–74.
10. Thysen S, Luyten FP, Lories RJ. Targets, models and challenges in osteoarthritis research. *Dis Model Mech* 2015;8:17–30.
11. Roos EM, Dahlberg L. Positive effects of moderate exercise on glycosaminoglycan content in knee cartilage: a four-month, randomized, controlled trial in patients at risk of osteoarthritis. *Arthritis Rheum* 2005;52:3507–14.
12. Galois L, Etienne S, Grossin L, Watrin-Pinzano A, Cournil-Henrionnet C, Loeuille D, et al. Dose–response relationship for exercise on severity of experimental osteoarthritis in rats: a pilot study. *Osteoarthritis Cartilage* 2004;12:779–86.
13. Ni GX, Lei L, Zhou YZ. Intensity-dependent effect of treadmill running on lubricin metabolism of rat articular cartilage. *Arthritis Res Ther* 2012;14:R256.
14. Loeser RF, Olex AL, McNulty MA, Carlson CS, Callahan M, Ferguson C, et al. Disease progression and phasic changes in gene expression in a mouse model of osteoarthritis. *PLoS One* 2013;8:e54633.
15. Nam J, Perera P, Liu J, Wu LC, Rath B, Butterfield TA, et al. Transcriptome-wide gene regulation by gentle treadmill walking during the progression of monoiodoacetate-induced arthritis. *Arthritis Rheum* 2011;63:1613–25.
16. Kilkenny C, Browne WJ, Cuthill IC, Emerson M, Altman DG. Improving bioscience research reporting: the ARRIVE guidelines for reporting animal research. *Osteoarthritis Cartilage* 2012;20:256–60.
17. Dishman RK, Armstrong RB, Delp MD, Graham RE, Dunn AL. Open-field behavior is not related to treadmill performance in exercising rats. *Physiol Behav* 1988;43:541–6.
18. Pritzker KP, Gay S, Jimenez SA, Ostergaard K, Pelletier JP, Revell PA, et al. Osteoarthritis cartilage histopathology: grading and staging. *Osteoarthritis Cartilage* 2006;14:13–29.
19. Botter SM, Glasson SS, Hopkins B, Clockaerts S, Weinans H, van Leeuwen JP, et al. ADAMTS5–/– mice have less subchondral bone changes after induction of osteoarthritis through surgical instability: implications for a link between cartilage and subchondral bone changes. *Osteoarthritis Cartilage* 2009;17:636–45.
20. Gerwin N, Bendele AM, Glasson S, Carlson CS. The OARS histopathology initiative – recommendations for histological assessments of osteoarthritis in the rat. *Osteoarthritis Cartilage* 2010;18(Suppl 3):S24–34.
21. Iijima H, Aoyama T, Ito A, Tajino J, Nagai M, Zhang X, et al. Destabilization of the medial meniscus leads to subchondral bone defects and site-specific cartilage degeneration in an experimental rat model. *Osteoarthritis Cartilage* 2014;22:1036–43.
22. Iijima H, Aoyama T, Ito A, Tajino J, Nagai M, Zhang X, et al. Immature articular cartilage and subchondral bone covered by menisci are potentially susceptible to mechanical load. *BMC Musculoskelet Disord* 2014;15:101.
23. Bobacz K, Gruber R, Soleiman A, Erlacher L, Smolen JS, Graninger WB. Expression of bone morphogenetic protein 6 in healthy and osteoarthritic human articular chondrocytes and

- stimulation of matrix synthesis in vitro. *Arthritis Rheum* 2003;48:2501–8.
24. Blaney Davidson EN, Vitters EL, van Lent PL, van de Loo FA, van den Berg WB, van der Kraan PM. Elevated extracellular matrix production and degradation upon bone morphogenetic protein-2 (BMP-2) stimulation point toward a role for BMP-2 in cartilage repair and remodeling. *Arthritis Res Ther* 2007;9:R102.
 25. Ishihara A, Shields KM, Litsky AS, Mattoon JS, Weisbrode SE, Bartlett JS, et al. Osteogenic gene regulation and relative acceleration of healing by adenoviral-mediated transfer of human BMP-2 or -6 in equine osteotomy and ostectomy models. *J Orthop Res* 2008;26:764–71.
 26. Cui Z, Xu C, Li X, Song J, Yu B. Treatment with recombinant lubricin attenuates osteoarthritis by positive feedback loop between articular cartilage and subchondral bone in ovariectomized rats. *Bone* 2015;74:37–47.
 27. Guzman RE, Evans MG, Bove S, Morenko B, Kilgore K. Monoiodoacetate-induced histologic changes in subchondral bone and articular cartilage of rat femorotibial joints: an animal model of osteoarthritis. *Toxicol Pathol* 2003;31:619–24.
 28. Botter SM, van Osch GJ, Clockaerts S, Waarsing JH, Weinans H, van Leeuwen JP. Osteoarthritis induction leads to early and temporal subchondral plate porosity in the tibial plateau of mice: an in vivo microfocus computed tomography study. *Arthritis Rheum* 2011;63:2690–9.
 29. Edd SN, Giori NJ, Andriacchi TP. The role of inflammation in the initiation of osteoarthritis after meniscal damage. *J Biomech* 2015;48:1420–6.
 30. Lockwood KA, Chu BT, Anderson MJ, Haudenschild DR, Christiansen BA. Comparison of loading rate-dependent injury modes in a murine model of post-traumatic osteoarthritis. *J Orthop Res* 2014;32:79–88.
 31. Pottenger LA, Phillips FM, Draganich LF. The effect of marginal osteophytes on reduction of varus–valgus instability in osteoarthritic knees. *Arthritis Rheum* 1990;33:853–8.
 32. Tochigi Y, Vaseenon T, Heiner AD, Fredericks DC, Martin JA, Rudert MJ, et al. Instability dependency of osteoarthritis development in a rabbit model of graded anterior cruciate ligament transection. *J Bone Joint Surg Am* 2011;93:640–7.
 33. Fukui N, Zhu Y, Maloney WJ, Clohisy J, Sandell LJ. Stimulation of BMP-2 expression by pro-inflammatory cytokines IL-1 and TNF-alpha in normal and osteoarthritic chondrocytes. *J Bone Joint Surg Am* 2003;85-A(Suppl 3):59–66.
 34. Dell'Accio F, De Bari C, El Tawil NM, Barone F, Mitsiadis TA, O'Dowd J, et al. Activation of WNT and BMP signaling in adult human articular cartilage following mechanical injury. *Arthritis Res Ther* 2006;8:R139.
 35. Hennig T, Lorenz H, Thiel A, Goetzke K, Dickhut A, Geiger F, et al. Reduced chondrogenic potential of adipose tissue derived stromal cells correlates with an altered TGFbeta receptor and BMP profile and is overcome by BMP-6. *J Cell Physiol* 2007;211:682–91.
 36. Sekiya I, Colter DC, Prockop DJ. BMP-6 enhances chondrogenesis in a subpopulation of human marrow stromal cells. *Biochem Biophys Res Commun* 2001;284:411–8.
 37. Sekiya I, Larson BL, Vuoristo JT, Reger RL, Prockop DJ. Comparison of effect of BMP-2, -4, and -6 on in vitro cartilage formation of human adult stem cells from bone marrow stroma. *Cell Tissue Res* 2005;320:269–76.
 38. Majumdar MK, Wang E, Morris EA. BMP-2 and BMP-9 promotes chondrogenic differentiation of human multipotential mesenchymal cells and overcomes the inhibitory effect of IL-1. *J Cell Physiol* 2001;189:275–84.
 39. Song K, Krause C, Shi S, Patterson M, Suto R, Grgurevic L, et al. Identification of a key residue mediating bone morphogenetic protein (BMP)-6 resistance to noggin inhibition allows for engineered BMPs with superior agonist activity. *J Biol Chem* 2010;285:12169–80.
 40. Li JZ, Li H, Sasaki T, Holman D, Beres B, Dumont RJ, et al. Osteogenic potential of five different recombinant human bone morphogenetic protein adenoviral vectors in the rat. *Gene Ther* 2003;10:1735–43.
 41. Zhu W, Rawlins BA, Boachie-Adjei O, Myers ER, Arimizu J, Choi E, et al. Combined bone morphogenetic protein-2 and -7 gene transfer enhances osteoblastic differentiation and spine fusion in a rodent model. *J Bone Miner Res* 2004;19:2021–32.
 42. Nakase T, Miyaji T, Tomita T, Kaneko M, Kuriyama K, Myoui A, et al. Localization of bone morphogenetic protein-2 in human osteoarthritic cartilage and osteophyte. *Osteoarthritis Cartilage* 2003;11:278–84.
 43. Lin W, Alizai H, Joseph GB, Srikkum W, Nevitt MC, Lynch JA, et al. Physical activity in relation to knee cartilage T2 progression measured with 3 T MRI over a period of 4 years: data from the Osteoarthritis Initiative. *Osteoarthritis Cartilage* 2013;21:1558–66.
 44. Yamaguchi S, Aoyama T, Ito A, Nagai M, Iijima H, Zhang X, et al. Effects of exercise level on biomarkers in a rat knee model of osteoarthritis. *J Orthop Res* 2013;31:1026–31.
 45. Assis L, Milares LP, Almeida T, Tim C, Magri A, Fernandes KR, et al. Aerobic exercise training and low-level laser therapy modulate inflammatory response and degenerative process in an experimental model of knee osteoarthritis in rats. *Osteoarthritis Cartilage* 2016;24:169–77.